

Hydroclimatic adaptation critical to the resilience of tropical forests

Chandrakant Singh^{1,2,*}, Ruud van der Ent^{3,4}, Lan Wang-Erlandsson^{1,2}, Ingo Fetzer^{1,2}

¹ Stockholm Resilience Centre, Stockholm University, Stockholm, Sweden

² Bolin Centre for Climate Research, Stockholm University, Stockholm, Sweden

³ Department of Water Management, Faculty of Civil Engineering and Geosciences, Delft University of Technology, Delft, The Netherlands

⁴ Department of Physical Geography, Faculty of Geosciences, Utrecht University, Utrecht, The Netherlands

* *Author to whom any correspondence should be addressed*

Contact information: chandrakant.singh@su.se

Running title: Empirical evidence to ecosystem's stability

ORCID

Chandrakant Singh: <http://orcid.org/0000-0001-9092-1855>

Ruud van der Ent: <https://orcid.org/0000-0001-5450-4333>

Lan Wang-Erlandsson: <http://orcid.org/0000-0002-7739-5069>

Ingo Fetzer: <http://orcid.org/0000-0001-7335-5679>

Abstract

Forest and savanna ecosystems naturally exist as alternative stable states. The maximum capacity of these ecosystems to absorb perturbations without transitioning to the other alternative stable state is referred to as 'resilience'. Previous studies have determined the resilience of terrestrial ecosystems to hydroclimatic changes predominantly based on space-for-time substitution. This substitution assumes that the contemporary spatial frequency distribution of ecosystems' tree cover structure holds across time. However, this assumption is problematic since ecosystem adaptation over time is ignored. Here we empirically study tropical forests' stability and hydroclimatic adaptation dynamics by examining remotely sensed tree cover change (ΔTC ; aboveground ecosystem structural change) and root zone storage capacity (S_r ; buffer capacity towards water-stress) over the last two decades. We find that ecosystems at high (>75%) and low (<10%) tree cover adapt by instigating considerable subsoil investment, and therefore experience limited ΔTC – signifying stability. In contrast, unstable ecosystems at intermediate (30-60%) tree cover are unable to exploit the same level of adaptation as stable ecosystems, thus showing considerable ΔTC . Ignoring this adaptive mechanism can underestimate the resilience of the forest ecosystems, which we find is largely underestimated in the case of the Congo rainforests. The results from this study emphasise the importance of the ecosystem's temporal dynamics and adaptation in inferring and assessing the risk of forest-savannah transitions under rapid hydroclimatic change.

Keyword: Alternative stable states; ecosystem change; forest-savanna transition; remote sensing; spatio-temporal approach; subsoil adaptation; transient state

1. Introduction

Climate change and deforestation reduces the resilience of rainforest ecosystems (Hirota et al., 2011; van Nes et al., 2016), and thus compromise their capacity to remain forests despite various perturbations (Davidson et al., 2012; Malhi et al., 2008). Resilience is quantified and analysed by constructing a ‘stability landscape’, in which valleys (‘basins of attraction’) represent ‘stable states’ and hilltops represent ‘unstable states’ under transition (Fig. 1). Resilience is then measured as the width of the basin of attraction around a stable state, which erodes towards bifurcation points (i.e., a point where stable and unstable states collide, becoming unstable) (Hirota et al., 2011; van Nes et al., 2016) (Fig. 1a). Within a basin of attraction, stabilising feedbacks help the ecosystem retain its structural and functional characteristics against perturbations (Holling, 1973). The ecosystem will eventually return to its native stable state (‘minimum’ of the basin) when perturbations on the system are released (Fig. 1b, c). Beyond a basin of attraction, however, i.e., trespassing a threshold (‘maximum’ of the basin), self-amplifying feedbacks will instead shift an ecosystem to an alternative stable state (Hirota et al., 2011; Holling, 1973). Therefore, a better understanding of stability and resilience is helpful to evaluate the potential of ecosystem adaptation and systemic risks under future (climatological or non-climatological) modifications to their conditions (Anderegg et al., 2020).

Due to the lack of analysis of dynamics through time series (Cole et al., 2014; Damgaard, 2019), our present understanding of the stability landscape of the tropical terrestrial ecosystems is based on the frequency distribution of tree cover (Dantas et al., 2016; Hirota et al., 2011; Staver et al., 2011a, 2011b), essentially making a space-for-time assumption (Fig. 1a). According to this assumption, the frequency distribution determines the size (i.e., width and depth) of the basin of attraction in the conceptual stability landscape, which is then interpreted to be ecosystems stability (deep basin, more stable and vice versa) and resilience (wider basin, more resilient and vice versa) across time (Scheffer et al., 2009) (Fig. 1a). However, temporal support to such ecosystem dynamics has not been investigated previously. The availability of longer time series of remote sensing data now allows for a better representation of these ecological states and resilience across time (Damgaard, 2019; Reyer et al., 2015).

Here, for the first time, to our knowledge, a time series of remotely sensed tree cover change (ΔTC) spanning two decades is analysed to investigate rainforest stability and resilience. It is well recognised that the ecosystem's response towards any perturbations is captured in the transient state of the ecosystem (Heimann & Reichstein, 2008; Turner et al., 2003; Wiczyński et al., 2019). Based on this, we hypothesise that the transient state of the ecosystem should resemble the stability landscape

found by the space-for-time assumption (Fig. 1a). Thus, a highly resilient ecosystem will not show considerable ΔTC over time, whereas a lowly resilient ecosystem will.

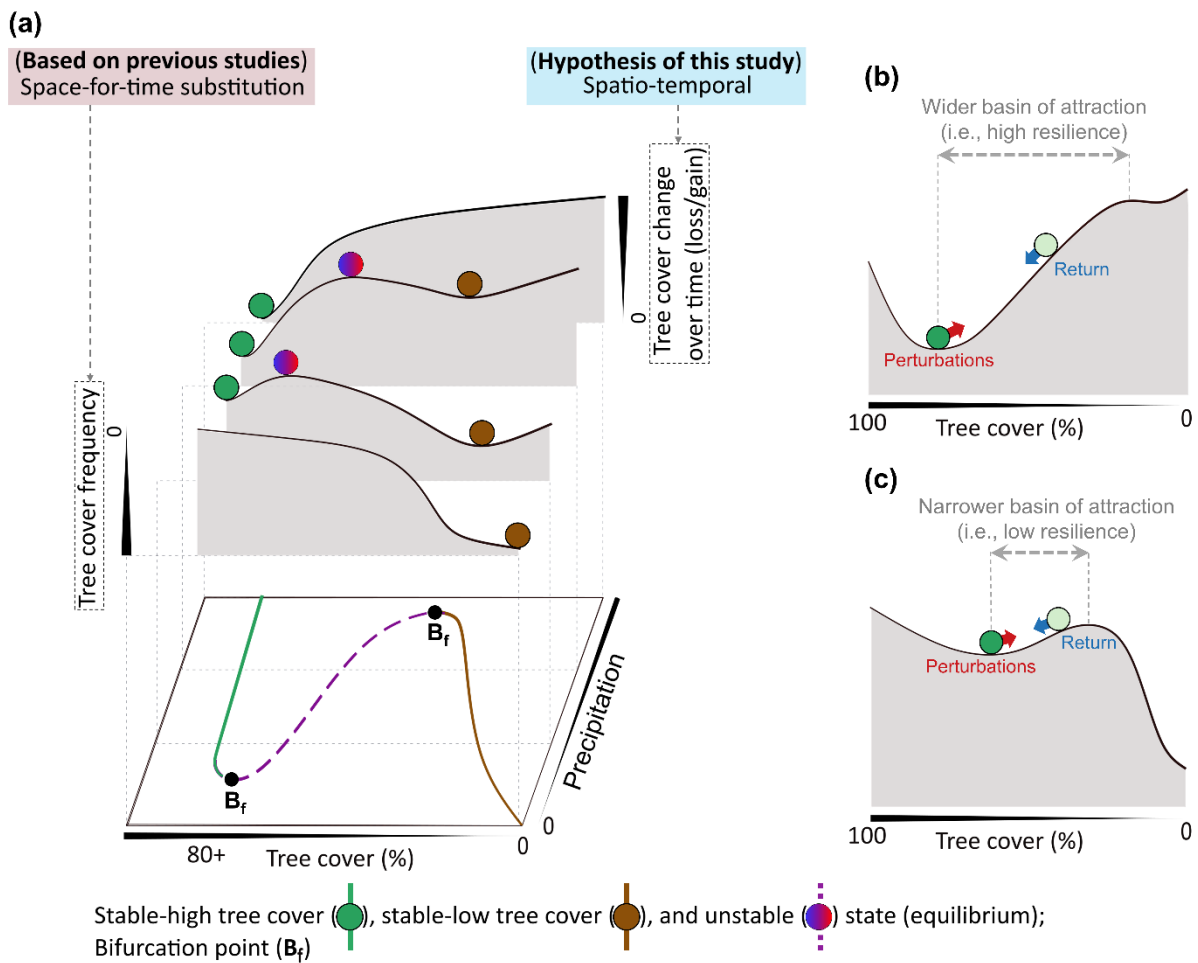


Fig. 1 | Stability landscape of ecosystems across different mean precipitation (mm yr^{-1}). (a) The landscape is, originally, based on the frequency distribution of the tree cover (space-for-time assumption (Dantas et al., 2016; Hirota et al., 2011; Staver et al., 2011a, 2011b)). This study substitutes ‘tree cover frequency’ with magnitudes of ‘tree cover change over time’ (spatio-temporal) for South America and Africa across different classes of precipitation, which we hypothesise should resemble the original landscape. Stable and unstable states (i.e., equilibria) correspond to the valleys (i.e., local minima) and hilltops (i.e., local maxima) in the stability landscapes, respectively. (b, c) Resilience of an individual ecosystem across the stability landscape is represented as the width of the basin of the attraction around a stable state, which declines towards the bifurcation points (i.e., a point where stable and unstable states collide; depicted in a). Perturbations push the ecosystem towards the hilltop, whereas the ecosystem returns to its stable state when these perturbations are released.

Our hypothesis suggests a correlation between ΔTC and resilience of the ecosystems. However, previous research overlooks any such correlation and only considers the hydroclimate – specifically mean precipitation (\bar{P}) – when quantifying forest resilience (Hirota et al., 2011; Staal et al., 2018).

Recent insights, however, hint towards the necessity to also incorporate the buffering capacity of the forest ecosystems, an aspect that is often lacking when representing the ecohydrology of tropical terrestrial ecosystems (Reyer et al., 2015; Singh et al., 2020; van Oorschot et al., 2021). By including root zone storage capacity (S_r), we account for the buffering capacity of the ecosystem in quantifying resilience. S_r represents the maximum amount of the subsoil moisture available to the ecosystems to buffer water deficit during dry periods (Wang-Erlandsson et al., 2016). This aspect acknowledges that ecosystems respond to water-stress (defined here as a deficit in soil water availability inhibiting plant growth) by actively investing in their above- and belowground structures to maximise their hydrological benefits (Migliavacca et al., 2021; Singh et al., 2020). Thus, the resulting resilience metric, by also explicitly considering the ecosystems' adaptive and buffering strategies, should be consistent with actual ΔTC .

2. Methods

2.1 Study area

This paper focuses on the tropical terrestrial ecosystems of South America and Africa, but the whole study area is slightly larger: 12°N-50°S for South America and 20°N-35°S for Africa. We have used a global administrative database from the Food and Agriculture Organisation (FAO; <http://www.fao.org/geonetwork/>) to define geographical boundaries for each country and do not have any political intentions behind our research.

2.2 Data

We used remotely sensed gauge-corrected precipitation and evaporation data for our analysis. The daily estimates of precipitation were obtained from the Climate Hazards Group InfraRed Precipitation with Station data (CHIRPS) (Funk et al., 2015) at 0.05° spatial resolution for the years 2000-2019. Furthermore, evaporation in this paper is defined as the sum of all evaporative moisture from the soil and terrestrial vegetation, including those from interception (Miralles et al., 2020). The evaporation datasets chosen for this study were free from any prior assumptions related to biome-dependent parameterisation (such as plant function types, stomatal conductance, maximum root allocation depth) and soil layer depth (represents maximum depth of moisture uptake) to avoid any artificially introduced transitions between different biomes. Furthermore, these datasets were either derived or validated from actual evaporation estimates (e.g., FLUXNET sites). These conditions narrowed our prospect of using the widely available evaporation datasets. Nevertheless, we created an equally-weighted ensemble of evaporation using three datasets: (i) Breathing Earth System Simulator (BESS) (Jiang & Ryu, 2016) (ii) Penman-Monteith-Leuning (PML) (Zhang et al., 2016), and (iii) FLUXCOM-

RS (Jung et al., 2019). While i and ii were obtained at 0.5°, iii was obtained at 0.083° spatial resolution. All three evaporation datasets were obtained at a monthly timescale for the years 2001-2012. We downscaled these datasets from monthly to daily timescale using the daily estimate of the ERA5 (Hersbach et al., 2020) evaporation at 0.25° spatial resolution.

The aboveground structure of the ecosystem was analysed using the remotely-sensed MOD44B (version 6) annual tree cover (TC) dataset (Dimiceli et al., 2017) at a fine resolution of 250 m × 250 m for the years 2000-2019. Here, a TC value of 50% would represent a ground coverage of 50% by the canopy in the whole pixel. Furthermore, to minimise the human influence on this analysis, we removed the pixels with human-influenced land use and non-terrestrial land cover using the European Space Agency's (ESA) Globcover land-use classification at 300 m resolution. Ultimately, all the mentioned above datasets were spatially interpolated to 250 m using bilinear interpolation, except for the land use dataset, which was interpolated using nearest-neighbour interpolation.

2.3 Spatio-temporal approach for determining ecosystem states

For evaluating these stable and unstable states, a sample size (n) of 1,000,000 pixels each – from both continents – from all the 250 m × 250 m pixels was chosen and analysed separately for South America and Africa. This sample was used to determine the tree cover change (ΔTC) in the ecosystem structure in the last two decades as follows:

$$\Delta TC = \overline{TC}_{2017-2019} - \overline{TC}_{2000-2002} \quad (1)$$

Where $\overline{TC}_{2017-2019}$ and $\overline{TC}_{2000-2002}$ represents the mean of the tree cover for the years 2017-2019 and 2000-2002, respectively. Then, we classified the sample (n) into four classes based on mean precipitation (\overline{P} ; Fig. 2a and c), with each \overline{P} class representing 25% of the total land area. We further separated each of these \overline{P} classes into tree cover gain (i.e., $\Delta TC \geq 0$) and tree cover loss ($\Delta TC < 0$) (Fig. 2a and c).

After classifying, we grouped the samples into separate bins sorted by mean tree cover (i.e., $\overline{TC}_{2000-2019}$; Fig. 2a and c), such that each bin represented an equal area (i.e., 2,500 sampled pixels = 156.25 km²). Lastly, to relate stable and unstable states with the ecosystem's structural change, the 13.4% of the bins with the highest change (i.e., highest ΔTC_{median}) from all the classes combined were categorised as unstable. Moreover, 38.2% of the bins with lowest change (i.e., lowest ΔTC_{median}) were

classified as stable. The justification behind selecting the stable and unstable regions was based on the area under the distribution curve (Supplementary Fig. 1).

These stable and unstable regions, which were analysed separately for tree cover gain and loss pixels at each \bar{P} class, were plotted spatially at 250 m resolution (Fig. 2). For example, our sample analysis suggests that the unstable region for tree cover loss in South America at \bar{P} class of 0-985 mm yr⁻¹ falls approximately between 40-60% $\overline{TC}_{2000-2019}$ (Fig. 2a). This will be spatially plotted in reality (population) for all the pixels falling between 40-60% $\overline{TC}_{2000-2019}$ at \bar{P} of 0-985 mm yr⁻¹ for the pixels where $\Delta TC < 0$.

2.4 Root zone storage capacity

For our analysis, we have considered root zone storage capacity (S_r ; derived from daily precipitation and evaporation data) to represent the adaptive buffer capacity of the ecosystem to absorb and adapt to water-stress conditions. S_r is the maximum amount of available subsurface moisture that vegetation can store and utilise through their roots for transpiration during dry periods (i.e., periods in which evaporation is greater than precipitation, irrespective of the seasons) (Gao et al., 2014; Wang-Erlandsson et al., 2016). Plants can increase their S_r by expanding their roots in the soil laterally as well as vertically. We adopted the mass-balance approach by Singh et al. (2020) to derive S_r from precipitation and evaporation estimates (Supplementary Method-1 in Supplementary Information). The underlying assumption of this approach is that ecosystems would not invest in expanding their storage capacity more than necessary to bridge the water-deficits it experiences (Wang-Erlandsson et al., 2016).

2.5 Forest resilience and validation

We adapted Hirota et al. (2011) methodology for determining resilience using logistic regressions (Supplementary Methods-3 in Supplementary Information). The logistic regression predicts the probability of forest (tree cover > 50%) as a function of the independent variable. Hirota et al. (2011) had only considered \bar{P} as the independent variable. However, the new resilience metric proposed in this study also considered S_r as an independent variable representing the drought buffer capacity of the forest ecosystems. Here, we experimented with \bar{P} and S_r independently and its combination, and chose the best performing model to represent the ecosystem state (Supplementary Table 1). We modified the S_r values for all the regions with tree cover < 30% to 99th percentile of each continent's S_r . This is because we assume that forest ecosystems will maximise their storage capacity (i.e., maximise

S_r) before transitioning to a savannah (Singh et al., 2020). Lastly, we validate the resilience estimates of \bar{P} and $\bar{P} + S_r$ combination for both tree cover loss and gain samples separately against observed ΔTC , and assess their performance using spearman rank correlation. A high positive or negative spearman correlation would indicate a high strength and consistency between the resilience estimates and ΔTC .

3. Results and discussion

3.1 Tree cover change in relation to stability equilibria

Our spatio-temporal analysis consistently shows low ΔTC for ecosystems at both high (>75%) and low (<10%) tree cover, whereas high ΔTC is observed for ecosystems at intermediate (30-60%) tree cover (Fig. 2a,c). A low ΔTC for both high and low tree cover ecosystems can be the result of either a minimal perturbation on the ecosystem over the last two decades (2000-2019), or a robust adaptive mechanism that is able to offset the experienced perturbations without considerable change in the ecosystem structure (Singh et al., 2020), which we, therefore, perceive as 'stable'. Conversely, a high ΔTC at intermediate tree cover (Fig. 2a,c) implies that the ecosystems in these ranges have been potentially influenced by either strong perturbations (Sutherland et al., 2018) (e.g., deforestation) causing significant changes to their ecosystem structure, or the adaptive mechanism under hydroclimatic changes has modified the ecosystem structure to utilise available resources efficiently. Since we exclude human influences, these high ΔTC can solely be explained by tree mortality under climate-induced water and fire stress (Staver et al., 2011a; van Nes et al., 2018) or tree growth under the influence of wetter climate (Holmgren et al., 2006), thus resulting in these ecosystems undergoing the observed regime shift (Hirota et al., 2011; Scheffer et al., 2009). The self-amplifying feedback between forest and climate also leads to considerable changes to ecosystem structure, such that forest loss facilitates dry conditions, and dry conditions further influence forest mortality (Staal et al., 2020; Zemp et al., 2017). Overall, structural changes to these ecosystems are much steeper than what we observed for ecosystems in their stable states (Fig. 2a,c). Thus, we consider such ecosystems as 'unstable'. These spatio-temporal patterns against different \bar{P} levels (Fig. 2a,c) further strengthen the presence of stability and instability in terrestrial ecosystems, which previous studies observed using a space-for-time assumption (Dantas et al., 2016; Hirota et al., 2011; Staver et al., 2011a, 2011b), can also manifest as actual ΔTC over time across the broader tree cover structures.

A closer look at these stable states (i.e., stable-low and -high tree cover bins representing a series of numerical ranges highlighted in dark brown and green, respectively, in Fig. 2a,c and spatially highlighted in Fig. 2b,d) reveals certain dissimilarities across the \bar{P} classes. Stable-high tree cover bins

decrease gradually with decreasing \bar{P} (Fig. 2a,c), thereby implying the inability of the forest ecosystems to maintain their dense structural characteristics under drier conditions (Singh et al., 2020). Here, an increase in ΔTC with decreasing \bar{P} suggests that these ecosystems are undergoing a shift to a savannah-like open-canopy structure due to intensifying water and fire stress (Hirota et al., 2011; Moser et al., 2010; Zemp et al., 2017). Reversely, stable-low tree cover bins decrease with increasing \bar{P} (Fig. 2a,c). Here, an increase in wetter conditions in the ecosystem helps suppress fire, thereby preventing fire-driven seedling mortality (Moser et al., 2010), and drives more soil water storage under a wetter climate (Guan et al., 2015). All these factors thus help promote forest growth and colonisation (Hirota et al., 2011; Uriarte et al., 2018). Nevertheless, the shifting potential, in both these cases, generally manifests itself as a relatively high ΔTC within the stable extent (e.g., relatively high ΔTC for $\bar{P} < 985 \text{ mm yr}^{-1}$ for South America, and $\bar{P} < 1,468 \text{ mm yr}^{-1}$ for Africa at a tree cover $> 70\%$ in Fig. 2), with some exceptions (Supplementary Fig. 3).

Interestingly, we also observe that for most of the \bar{P} classes, the extent of the unstable bins (i.e., ranges highlighted in red and blue in Fig. 2a, c) is almost similar for both tree cover loss and gain segments. In contrast to stable states, higher potential – suggesting amplified feedback – for both tree cover loss and gain at intermediate tree cover was already hypothesised in a space-for-time based approach (Hirota et al., 2011) (Fig. 1a) and is confirmed by observable evidence at field scale. For example, open forest structure is promoted under increasingly drier conditions (McAlpine et al., 2018), influence of fire (Pivello et al., 2021) and fragmentation (Nikonovas et al., 2020). Whereas, forest growth is promoted under El Niño-southern oscillation influenced wet conditions (Gutiérrez et al., 2008; Holmgren et al., 2006), sustainable management (Chazdon et al., 2020; Lewis et al., 2019; Wilson et al., 2019) and conservation efforts undertaken by local authorities to reduce deforestation, extensive grazing and wildfires (Cheung et al., 2010; Guedes Pinto & Voivodic, 2021; Sánchez-Cuervo et al., 2012)).

Our spatio-temporal approach provides empirical evidence to this ΔTC potential at continental scales, as well as proves that the ecosystem change leading to a regime shift – in context of both tree cover loss and gain – is indeed intensified at intermediate tree cover (Hirota et al., 2011) (Fig. 2). This change in tree cover structure (ΔTC) across different \bar{P} levels, thus, agrees with our spatio-temporal hypothesis (Fig. 1a and 2). Furthermore, spatially mapping these stable and unstable states provides us with key regions where forest conservation and management efforts need to be strengthened.

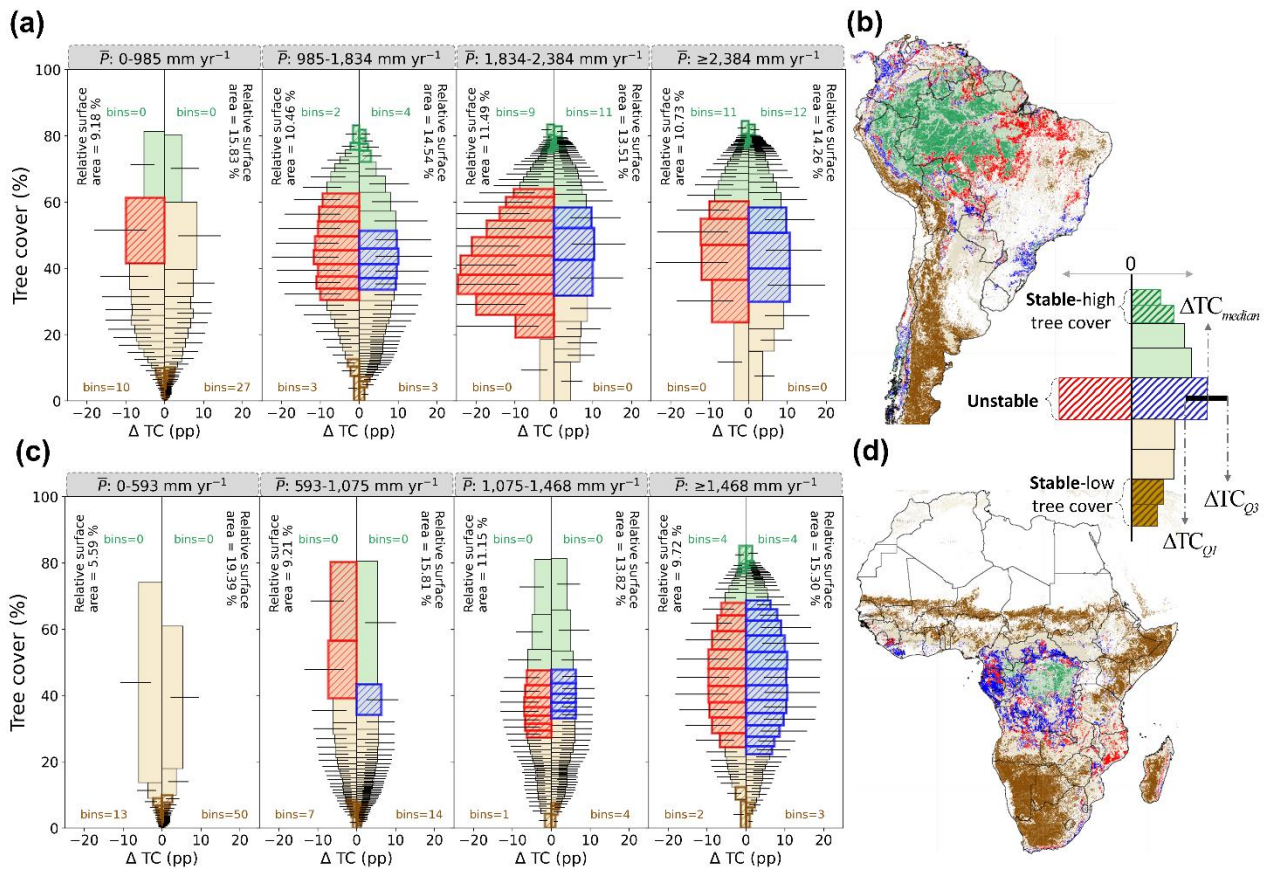


Fig. 2 | Determining the stability landscape of the tropical terrestrial ecosystem. The landscape for (a, b) South America and (c, d) Africa are analysed using the tree cover (%), tree cover change (ΔTC ; percent point (pp)) over the last two decades (from 2000-2019; see methods), and mean precipitation (\bar{P} (mm yr^{-1}); from 2000-2019). The total samples are equally divided into four \bar{P} classes. Here, each individual bin within each \bar{P} class corresponds to 2,500 samples. From all these bins, the one with the least ΔTC is considered stable, and the one with the most ΔTC is unstable (see methods). These stable bins at low (dark brown) and high (dark green) tree cover in (a, c) are spatially plotted in (b, d). The unstable bins on either side of $\Delta TC = 0$ correspond to tree cover loss (red) or gain (blue). The relative surface area in (a, c) represents the portion of total sample surface area (separately for South America and Africa) on either side of the $\Delta TC = 0$. The tree cover extent of stable and unstable bins in (a, c) are spatially plotted in (b, d). The white regions in (b, d) correspond to excluded land cover (Supplementary Fig. 2d). High resolution maps of (b,d) can also be visualised at the Google Earth Engine (<https://chandrakant.users.earthengine.app/view/state-of-ecosystem>).

3.2 Forest stability and adaptation dynamics

But why can forest ecosystems maintain stability at different \bar{P} levels and how does that relate to ΔTC (Fig. 2)? The results from our S_r analysis suggest that forest ecosystems maintain their tree cover structure at decreasing \bar{P} by increasing investment in their subsoil structure (Fig. 3). Here, we observe a steep increase in S_r with both decreasing \bar{P} and tree cover (Fig. 3). In South America, within the

stability extent of tree cover from 85-75%, the S_r increases up to 600 mm with decreasing \bar{P} (Fig. 3a). For Africa, although only a small portion of the forest is in this comparatively low S_r high-tree cover stable state, we still observe a steep increase in S_r near the stable-high tree cover state with decreasing \bar{P} (Fig. 3b). The least ΔTC within this stability extent reveals that stabilising feedbacks within the stable-high tree cover (forest) ecosystems' respond to the change in \bar{P} by instigating S_r investment (Fig. 2 and 3). This S_r investment, in reality, is the vertical and lateral growth of roots, allowing for more subsoil moisture storage. This subsoil storage thereby assists the forest ecosystems in maintaining their (stable) dense tree cover structure even under hydroclimatic stresses (Schenk & Jackson, 2002; Singh et al., 2020). However, this stabilising feedback of S_r investment to keep the ecosystems in a stable-high tree cover state starts to change as we move to the intermediate tree cover.

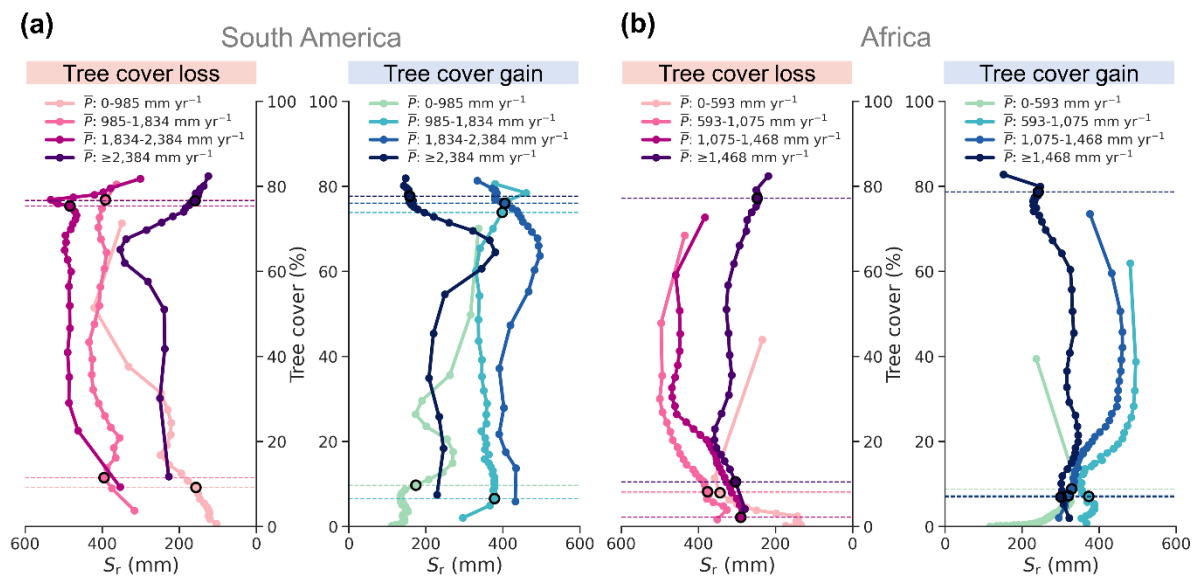


Fig. 3 | Relationship between mean precipitation (\bar{P}) and root zone storage capacity (S_r) for (a) South America and (b) Africa. The solid lines correspond to median S_r for the bins of tree cover loss (left) and gain (right) in Fig. 2. The points on the solid lines represent the centre of the individual bins. The (horizontal) dashed lines correspond to the minimum and maximum extent of the stable-high and -low tree cover ecosystems, respectively, as defined in Fig. 2a, c.

At (unstable) intermediate tree cover, we find ΔTC to gradually increase and maximise around 40-50% tree cover (Fig. 2). We also find that the steep increase in S_r gradually maximises around the 70-60% tree cover and remains unchanged between 60-30% tree cover (Fig. 3), thus suggesting causation between maximum S_r investment and changes to ecosystem structure. When analysing the changes to the forest ecosystems' structure against varying levels of drought and fire stress at the local scale (Supplementary Fig. 4 and 5), we observe that unstable state forests – in comparison to stable-

high tree cover ecosystems – have often maximised their S_r investment and show deterioration to a savannah-like state.

These deteriorations are not sudden but gradual over time. This suggests that there exists a certain maximum investment potential beyond which the shift from forest to a savannah state becomes eminent (Singh et al., 2020), which manifests itself as relatively high rate of ΔTC over time for the unstable forest ecosystems (Fig. 2, Supplementary Fig. 4 and 5). Considering S_r along with \bar{P} , therefore, has allowed us to evaluate the invisible buffering responses of forest ecosystems which otherwise are not apparent but are critical to the stability of the forest ecosystems. Overall, these responses are specifically catered towards efficiently optimising the available water resources and modifying ecosystem's aboveground tree cover structure (Migliavacca et al., 2021), and thus is able to manifest the shifts between the transient (stable and unstable) states as different magnitudes of ΔTC .

3.3 Resilience of the rainforest

This study quantifies resilience using logistic regression that predicts the probability of the occurrence of a forest ecosystem (tree cover > 50%) as a function of both \bar{P} and S_r for respective continents (Supplementary Table 1 and 2). It predicts resilience between a scale of 0 to 1, where 1 represents the highest probability of finding forest – interpreted as highly resilient forest ecosystem against perturbations – given the \bar{P} and S_r estimates in the recent decades. Fig. 4 shows that the most resilient forests are located in the central and central-western parts of Amazon rainforests in South America, and a major portion of the central Congo rainforests in Africa. At the same time, the least resilient forests are in the central-eastern and southern corridor of the Amazon rainforest (along the 'Amazonian arc of deforestation'); and northern and southern parts of the Congo rainforest (Fig. 4).

The $\bar{P} + S_r$ -based resilience metric shows that the resilience of a large portion of the Congo rainforest is higher than previously presumed (based on \bar{P} only) (Hirota et al., 2011; Staal et al., 2018), whereas the resilience of Amazon rainforests shows minor differences (Fig. 4 and Supplementary Fig. 6). Due to the unique evolutionary history of their respective ecology and climatology (Morley, 2000), high wet-season precipitation has allowed for Amazonian rainforests species to have a larger subsoil storage (i.e., S_r) to buffer the water-deficit than the Congo rainforests (Guan et al., 2015; Zhou et al., 2014). The grass species in Congo rainforests, on the other hand, have evolved to be highly water-efficient (Still et al., 2003). This reduces the competitiveness between trees and grasses for moisture uptake (Singh et al., 2020), thereby increasing the resilience of the overall Congo rainforest ecosystem, even with low S_r , against water-deficit. Therefore, including S_r in our resilience metric has allowed us to

capture this grass species-induced drought coping strategy in Congo rainforests, which otherwise is hard to detect with just \bar{P} . Nevertheless, the resilience of both these rainforest ecosystems are declining due to increasing regional climatic risks (Phillips et al., 2009), and combined feedbacks from local deforestation and human-induced fires (Davidson et al., 2012; Malhi et al., 2008).

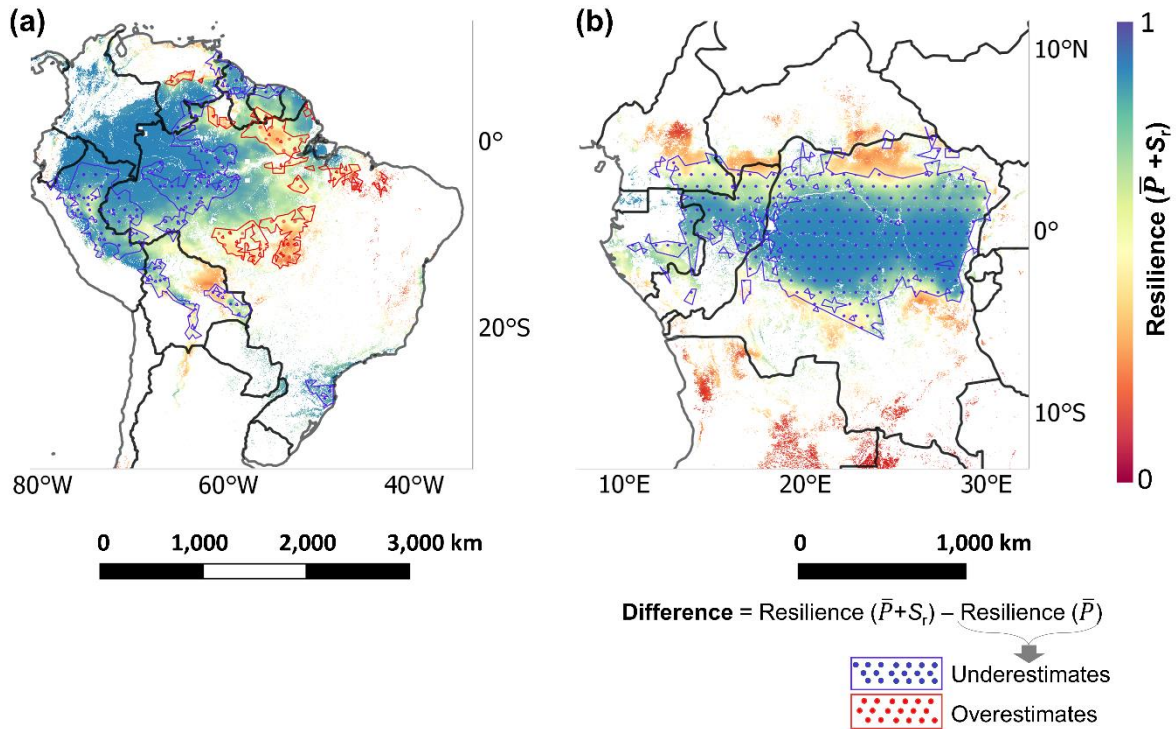


Fig. 4 | Resilience of the rainforest ecosystem. These resilience estimates are derived using the logistic regression based on \bar{P} and S_r for both (a) South America and (b) Africa. Here, a value of ‘1’ implies a forest ecosystem with highest resilience, and ‘0’ implies a forest ecosystem with lowest resilience. Comparing the two resilience metrics, we observed that by considering only \bar{P} (in resilience calculation), the resilience estimates show considerable differences for the Amazon and Congo rainforests (exact difference in Supplementary Fig. 6). Regions with tree cover $\leq 50\%$ and human-influenced land use (see methods) are masked.

Validation with actual ΔTC shows that the $\bar{P} + S_r$ -based resilience estimates perform better than only the \bar{P} -based resilience (Fig. 5). The performance of these resilience metrics based on ΔTC further strengthens our original hypothesis that more resilient ecosystems will tend to have lower ΔTC and vice versa (Fig. 1a and Fig. 5). Although \bar{P} is an important variable defining the broad influence of moisture on the ecohydrology of the ecosystem, considering S_r accounts for the local-scale ecosystem adaptation of forests to buffer and withstand hydroclimatic changes (Singh et al., 2020), and is thus able to better represent the resilience of the rainforest ecosystems (Supplementary Table 1). This better

representation of ecosystem resilience can play a crucial role in management and conservation efforts (Newton, 2016).

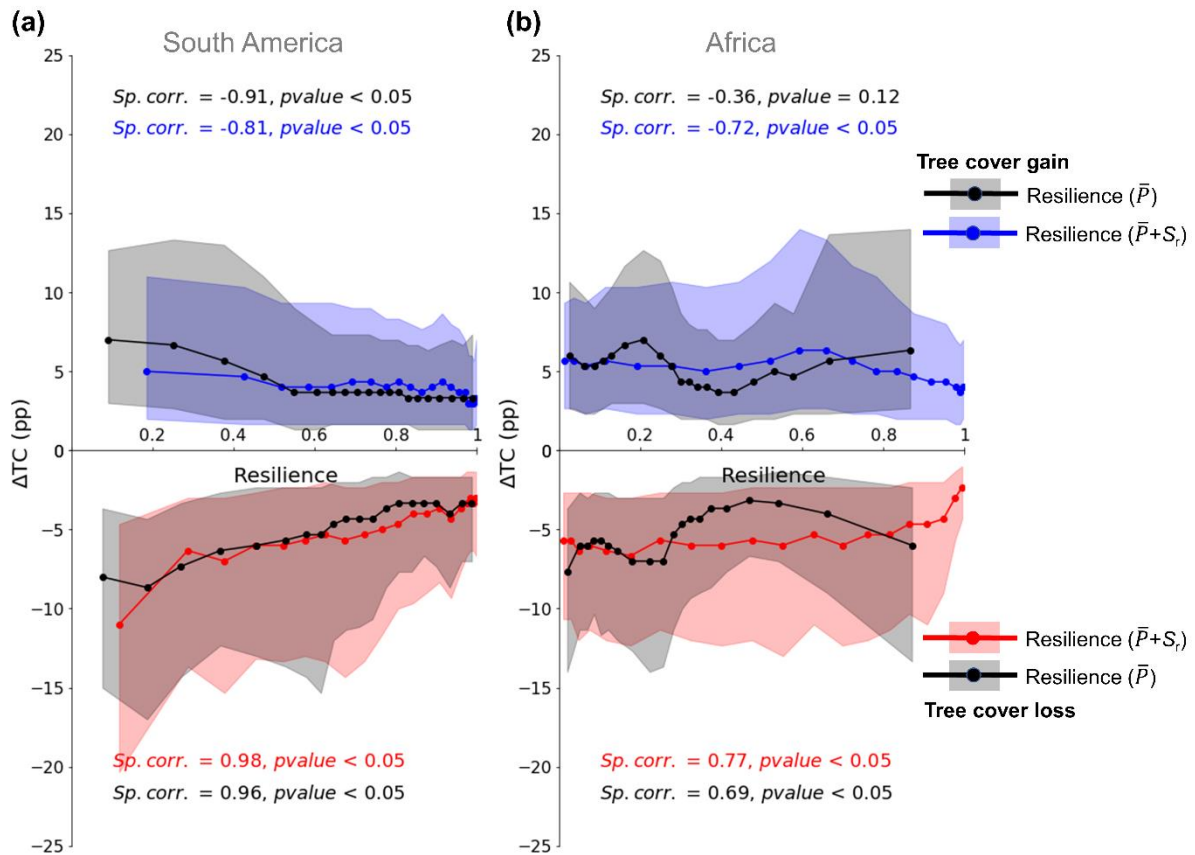


Fig. 5 | Validating the resilience estimates of the rainforest ecosystem with actual tree cover change (ΔTC) for (a) South America and (b) Africa. The samples are divided into 20 equally weighted intervals (similar to Fig. 2). The dots in blue (i.e., $\Delta TC \geq 0$) and red (i.e., $\Delta TC < 0$) correspond to our (\bar{P} and S_r) resilience metric, whereas dots in black correspond to \bar{P} -derived resilience estimates. The shaded regions represent the 1st and 3rd quantile. The statistical test calculates the spearman rank correlation (*Sp. corr.*) coefficient with associated p-value.

4. Conclusions

We demonstrate that our observation-based spatio-temporal approach, which analyses ΔTC and S_r over the last two decades, provides empirical evidence to alternative stable states in the tropical terrestrial ecosystem of South America and Africa. We observe that the stable ecosystems at $> 75\%$ and $< 10\%$ tree cover show low ΔTC by instigating higher S_r investment. For stable ecosystems, S_r investment does not come at the expense of changes in aboveground forest structure. Compared to stable ecosystems, unstable ecosystems show much high ΔTC manifesting at intermediate tree cover of 30–60% due to the inability of the ecosystems to utilise a similar level of investment. These tree cover

ranges of stability and instability resemble the stability landscape of the previous space-for-time substitution-based approach.

By only considering \bar{P} , the resilience of the ecosystems can be underestimated, which we observe for a considerable portion in the Congo rainforests. Only by modifying the existing, commonly used \bar{P} -based resilience metric with an extended $\bar{P}+S_r$ metric, we account for both the influence of hydroclimate (i.e., \bar{P}) and the hydroclimatic adaptive capacity of the ecosystem (i.e., S_r). Furthermore, the $\bar{P}+S_r$ resilience metric shows better performance, and consistency with actual ΔTC , thus strengthening its performance over the \bar{P} -based metric. Overall, this study accounts for the ecosystems temporal and adaptation dynamics which are becoming increasingly important to assess the transient state of the ecosystems under rapidly changing hydroclimatic conditions.

Data availability statement

The python and google earth engine code used for the analyses presented in this study is available from GitHub: <https://github.com/chandrakant6492/Ecosystems-stability-and-resilience>. The python code for calculating root zone storage capacity is also available from GitHub: <https://github.com/chandrakant6492/Drought-coping-strategy>. The resilience maps generated for this study are available at Zenodo: <https://doi.org/10.5281/zenodo.5878792>. Other publicly available datasets that support the findings of this study are available at: (P-CHIRPS) <https://data.chc.ucsb.edu/products/CHIRPS-2.0/>, (E-BESS) <ftp://147.46.64.183/>, (E-FLUXCOM) <ftp.bgc-jena.mpg.de>, (E-PML) <https://data.csiro.au/collections/#collection/CiCSIRO:17375v2>, (MOD44B_v6) <https://lpdaac.usgs.gov/products/mod44bv006/>, (Globcover) http://due.esrin.esa.int/page_globcover.php, (SPEI) <https://spei.csic.es/database.html>, (FireCCI51) https://geogra.uah.es/fire_cci/firecci51.php.

Acknowledgements

CS, LWE and IF acknowledge funding from the European Research Council (ERC) project 'Earth Resilience in the Anthropocene (ERA)', project number ERC-2016-ADG-743080. LWE also acknowledges funding from the Swedish Research Council for Sustainable Development (FORMAS), project number 2019-01220. RE acknowledges funding from the Netherlands Organization for Scientific Research (NWO), project number 016.Veni.181.015.

Competing interests

The authors declare no competing interests.

Supplementary Information is openly available at Global Change Biology (<https://onlinelibrary.wiley.com/doi/10.1111/gcb.16115>)

References

- Anderegg, W. R. L., Trugman, A. T., Badgley, G., Konings, A. G., & Shaw, J. (2020). Divergent forest sensitivity to repeated extreme droughts. *Nature Climate Change*, *10*(12), 1091–1095. <https://doi.org/10.1038/s41558-020-00919-1>
- Chazdon, R. L., Lindenmayer, D., Guariguata, M. R., Crouzeilles, R., Benayas, J. M. R., & Chaverro, E. L. (2020). Fostering natural forest regeneration on former agricultural land through economic and policy interventions. *Environmental Research Letters*, *15*(4), 043002. <https://doi.org/10.1088/1748-9326/ab79e6>
- Cheung, K. C., Liebsch, D., & Marques, M. C. M. (2010). Forest Recovery in Newly Abandoned Pastures in Southern Brazil: Implications for the Atlantic Rain Forest Resilience. *Natureza & Conservação*, *08*(01), 66–70. <https://doi.org/10.4322/natcon.00801010>
- Cole, L. E. S., Bhagwat, S. A., & Willis, K. J. (2014). Recovery and resilience of tropical forests after disturbance. *Nature Communications*, *5*(1), 3906. <https://doi.org/10.1038/ncomms4906>
- Damgaard, C. (2019). A Critique of the Space-for-Time Substitution Practice in Community Ecology. *Trends in Ecology & Evolution*, *34*(5), 416–421. <https://doi.org/10.1016/j.tree.2019.01.013>
- Dantas, V. de L., Hirota, M., Oliveira, R. S., & Pausas, J. G. (2016). Disturbance maintains alternative biome states. *Ecology Letters*, *19*(1), 12–19. <https://doi.org/10.1111/ele.12537>
- Davidson, E. A., de Araújo, A. C., Artaxo, P., Balch, J. K., Brown, I. F., C. Bustamante, M. M., Coe, M. T., DeFries, R. S., Keller, M., Longo, M., Munger, J. W., Schroeder, W., Soares-Filho, B. S., Souza, C. M., & Wofsy, S. C. (2012). The Amazon basin in transition. *Nature*, *481*(7381), 321–328. <https://doi.org/10.1038/nature10717>
- Dimiceli, C., Carroll, M., Sohlberg, R., Kim, D. H., & Kelly, M. (2017). *MOD44B MODIS/Terra Vegetation Continuous Fields Yearly L3 Global 250m SIN Grid V006* [Data set]. NASA EOSDIS Land Processes DAAC. <https://doi.org/10.5067/MODIS/MOD44B.006>
- Funk, C., Peterson, P., Landsfeld, M., Pedreros, D., Verdin, J., Shukla, S., Husak, G., Rowland, J., Harrison, L., Hoell, A., & Michaelsen, J. (2015). The climate hazards infrared precipitation with stations— A new environmental record for monitoring extremes. *Scientific Data*, *2*(1), 150066. <https://doi.org/10.1038/sdata.2015.66>
- Gao, H., Hrachowitz, M., Schymanski, S. J., Fenicia, F., Sriwongsitanon, N., & Savenije, H. H. G. (2014). Climate controls how ecosystems size the root zone storage capacity at catchment scale: Root zone storage capacity in catchments. *Geophysical Research Letters*, *41*(22), 7916–7923. <https://doi.org/10.1002/2014GL061668>
- Guan, K., Pan, M., Li, H., Wolf, A., Wu, J., Medvigy, D., Caylor, K. K., Sheffield, J., Wood, E. F., Malhi, Y., Liang, M., Kimball, J. S., Saleska, S. R., Berry, J., Joiner, J., & Lyapustin, A. I. (2015). Photosynthetic seasonality of global tropical forests constrained by hydroclimate. *Nature Geoscience*, *8*(4), 284–289. <https://doi.org/10.1038/ngeo2382>
- Guedes Pinto, L. F., & Voivodic, M. (2021). Reverse the tipping point of the Atlantic Forest for mitigation. *Nature Climate Change*, *11*(5), 364–365. <https://doi.org/10.1038/s41558-021-01035-4>
- Gutiérrez, A. G., Barbosa, O., Christie, D. A., Del-Val, E., Ewing, H. A., Jones, C. G., Marquet, P. A., Weathers, K. C., & Armesto, J. J. (2008). Regeneration patterns and persistence of the fog-dependent Fray Jorge forest in semiarid Chile during the past two centuries. *Global Change Biology*, *14*(1), 161–176. <https://doi.org/10.1111/j.1365-2486.2007.01482.x>
- Heimann, M., & Reichstein, M. (2008). Terrestrial ecosystem carbon dynamics and climate feedbacks. *Nature*, *451*(7176), 289–292. <https://doi.org/10.1038/nature06591>
- Hersbach, H., Bell, B., Berrisford, P., Hirahara, S., Horányi, A., Muñoz-Sabater, J., Nicolas, J., Peubey, C., Radu, R., Schepers, D., Simmons, A., Soci, C., Abdalla, S., Abellan, X., Balsamo, G., Bechtold, P., Biavati, G., Bidlot, J., Bonavita, M., ... Thépaut, J.-N. (2020). The ERA5 Global Reanalysis. *Quarterly Journal of the Royal Meteorological Society*, *245*(n/a), 111840. <https://doi.org/10.1002/qj.3803>

- Hirota, M., Holmgren, M., Van Nes, E. H., & Scheffer, M. (2011). Global Resilience of Tropical Forest and Savanna to Critical Transitions. *Science*, *334*(6053), 232–235. <https://doi.org/10.1126/science.1210657>
- Holling, C. S. (1973). Resilience and Stability of Ecological Systems. *Annual Review of Ecology and Systematics*, *4*(1), 1–23. <https://doi.org/10.1146/annurev.es.04.110173.000245>
- Holmgren, M., López, B. C., Gutiérrez, J. R., & Squeo, F. A. (2006). Herbivory and plant growth rate determine the success of El Niño Southern Oscillation-driven tree establishment in semiarid South America. *Global Change Biology*, *12*(12), 2263–2271. <https://doi.org/10.1111/j.1365-2486.2006.01261.x>
- Jiang, C., & Ryu, Y. (2016). Multi-scale evaluation of global gross primary productivity and evapotranspiration products derived from Breathing Earth System Simulator (BESS). *Remote Sensing of Environment*, *186*, 528–547. <https://doi.org/10.1016/j.rse.2016.08.030>
- Jung, M., Koirala, S., Weber, U., Ichii, K., Gans, F., Camps-Valls, G., Papale, D., Schwalm, C., Tramontana, G., & Reichstein, M. (2019). The FLUXCOM ensemble of global land-atmosphere energy fluxes. *Scientific Data*, *6*(1), 74. <https://doi.org/10.1038/s41597-019-0076-8>
- Lewis, S. L., Wheeler, C. E., Mitchard, E. T. A., & Koch, A. (2019). Restoring natural forests is the best way to remove atmospheric carbon. *Nature*, *568*(7750), 25–28. <https://doi.org/10.1038/d41586-019-01026-8>
- Malhi, Y., Roberts, J. T., Betts, R. A., Killeen, T. J., Li, W., & Nobre, C. A. (2008). Climate Change, Deforestation, and the Fate of the Amazon. *Science*, *319*(5860), 169–172. <https://doi.org/10.1126/science.1146961>
- McAlpine, C. A., Johnson, A., Salazar, A., Syktus, J., Wilson, K., Meijaard, E., Seabrook, L., Dargusch, P., Nordin, H., & Sheil, D. (2018). Forest loss and Borneo’s climate. *Environmental Research Letters*, *13*(4), 044009. <https://doi.org/10.1088/1748-9326/aaa4ff>
- Migliavacca, M., Musavi, T., Mahecha, M. D., Nelson, J. A., Knauer, J., Baldocchi, D. D., Perez-Priego, O., Christiansen, R., Peters, J., Anderson, K., Bahn, M., Black, T. A., Blanken, P. D., Bonal, D., Buchmann, N., Caldararu, S., Carrara, A., Carvalhais, N., Cescatti, A., ... Reichstein, M. (2021). The three major axes of terrestrial ecosystem function. *Nature*, 1–5. <https://doi.org/10.1038/s41586-021-03939-9>
- Miralles, D. G., Brutsaert, W., Dolman, A. J., & Gash, J. H. (2020). On the Use of the Term “Evapotranspiration.” *Water Resources Research*, *56*(11), e2020WR028055. <https://doi.org/10.1029/2020WR028055>
- Morley, R. J. (2000). *Origin and evolution of tropical rain forests*. John Wiley & Sons. <https://www.cabdirect.org/cabdirect/abstract/20000612672>
- Moser, B., Temperli, C., Schneiter, G., & Wohlgemuth, T. (2010). Potential shift in tree species composition after interaction of fire and drought in the Central Alps. *European Journal of Forest Research*, *129*(4), 625–633. <https://doi.org/10.1007/s10342-010-0363-6>
- Newton, A. C. (2016). Biodiversity Risks of Adopting Resilience as a Policy Goal. *Conservation Letters*, *9*(5), 369–376. <https://doi.org/10.1111/conl.12227>
- Nikonovas, T., Spessa, A., Doerr, S. H., Clay, G. D., & Mezbahuddin, S. (2020). Near-complete loss of fire-resistant primary tropical forest cover in Sumatra and Kalimantan. *Communications Earth & Environment*, *1*(1), 1–8. <https://doi.org/10.1038/s43247-020-00069-4>
- Phillips, O. L., Aragão, L. E. O. C., Lewis, S. L., Fisher, J. B., Lloyd, J., López-González, G., Malhi, Y., Monteagudo, A., Peacock, J., Quesada, C. A., Heijden, G. van der, Almeida, S., Amaral, I., Arroyo, L., Aymard, G., Baker, T. R., Bánki, O., Blanc, L., Bonal, D., ... Torres-Lezama, A. (2009). Drought Sensitivity of the Amazon Rainforest. *Science*, *323*(5919), 1344–1347. <https://doi.org/10.1126/science.1164033>
- Pivello, V. R., Vieira, I., Christianini, A. V., Ribeiro, D. B., da Silva Menezes, L., Berlinck, C. N., Melo, F. P. L., Marengo, J. A., Tornquist, C. G., Tomas, W. M., & Overbeck, G. E. (2021). Understanding Brazil’s catastrophic fires: Causes, consequences and policy needed to prevent future

- tragedies. *Perspectives in Ecology and Conservation*, 19(3), 233–255. <https://doi.org/10.1016/j.pecon.2021.06.005>
- Reyer, C. P. O., Brouwers, N., Rammig, A., Brook, B. W., Epila, J., Grant, R. F., Holmgren, M., Langerwisch, F., Leuzinger, S., Lucht, W., Medlyn, B., Pfeifer, M., Steinkamp, J., Vanderwel, M. C., Verbeeck, H., & Vilella, D. M. (2015). Forest resilience and tipping points at different spatio-temporal scales: Approaches and challenges. *Journal of Ecology*, 103(1), 5–15. <https://doi.org/10.1111/1365-2745.12337>
- Sánchez-Cuervo, A. M., Aide, T. M., Clark, M. L., & Etter, A. (2012). Land Cover Change in Colombia: Surprising Forest Recovery Trends between 2001 and 2010. *PLOS ONE*, 7(8), e43943. <https://doi.org/10.1371/journal.pone.0043943>
- Scheffer, M., Bascompte, J., Brock, W. A., Brovkin, V., Carpenter, S. R., Dakos, V., Held, H., van Nes, E. H., Rietkerk, M., & Sugihara, G. (2009). Early-warning signals for critical transitions. *Nature*, 461(7260), 53–59. <https://doi.org/10.1038/nature08227>
- Schenk, H. J., & Jackson, R. B. (2002). Rooting depths, lateral root spreads and below-ground/above-ground allometries of plants in water-limited ecosystems. *Journal of Ecology*, 90(3), 480–494. <https://doi.org/10.1046/j.1365-2745.2002.00682.x>
- Singh, C., Wang-Erlandsson, L., Fetzer, I., Rockström, J., & Ent, R. van der. (2020). Rootzone storage capacity reveals drought coping strategies along rainforest-savanna transitions. *Environmental Research Letters*, 15(12), 124021. <https://doi.org/10.1088/1748-9326/abc377>
- Staal, A., Flores, B. M., Aguiar, A. P. D., Bosmans, J. H. C., Fetzer, I., & Tuinenburg, O. A. (2020). Feedback between drought and deforestation in the Amazon. *Environmental Research Letters*, 15(4), 044024. <https://doi.org/10.1088/1748-9326/ab738e>
- Staal, A., Tuinenburg, O. A., Bosmans, J. H. C., Holmgren, M., van Nes, E. H., Scheffer, M., Zemp, D. C., & Dekker, S. C. (2018). Forest-rainfall cascades buffer against drought across the Amazon. *Nature Climate Change*, 8(6), 539–543. <https://doi.org/10.1038/s41558-018-0177-y>
- Staver, A. C., Archibald, S., & Levin, S. (2011a). Tree cover in sub-Saharan Africa: Rainfall and fire constrain forest and savanna as alternative stable states. *Ecology*, 92(5), 1063–1072. <https://doi.org/10.1890/10.1684.1>
- Staver, A. C., Archibald, S., & Levin, S. A. (2011b). The Global Extent and Determinants of Savanna and Forest as Alternative Biome States. *Science*, 334(6053), 230–232. <https://doi.org/10.1126/science.1210465>
- Still, C. J., Berry, J. A., Collatz, G. J., & DeFries, R. S. (2003). Global distribution of C3 and C4 vegetation: Carbon cycle implications. *Global Biogeochemical Cycles*, 17(1), 6-16–14. <https://doi.org/10.1029/2001GB001807>
- Sutherland, I. J., Villamagna, A. M., Dallaire, C. O., Bennett, E. M., Chin, A. T. M., Yeung, A. C. Y., Lamothe, K. A., Tomscha, S. A., & Cormier, R. (2018). Undervalued and under pressure: A plea for greater attention toward regulating ecosystem services. *Ecological Indicators*, 94, 23–32. <https://doi.org/10.1016/j.ecolind.2017.06.047>
- Turner, M. G., Collins, S. L., Lugo, A. L., Magnuson, J. J., Rupp, T. S., & Swanson, F. J. (2003). Disturbance Dynamics and Ecological Response: The Contribution of Long-Term Ecological Research. *BioScience*, 53(1), 46–56. [https://doi.org/10.1641/0006-3568\(2003\)053\[0046:DDAERT\]2.0.CO;2](https://doi.org/10.1641/0006-3568(2003)053[0046:DDAERT]2.0.CO;2)
- Uriarte, M., Muscarella, R., & Zimmerman, J. K. (2018). Environmental heterogeneity and biotic interactions mediate climate impacts on tropical forest regeneration. *Global Change Biology*, 24(2), e692–e704. <https://doi.org/10.1111/gcb.14000>
- van Nes, E. H., Arani, B. M. S., Staal, A., van der Bolt, B., Flores, B. M., Bathiany, S., & Scheffer, M. (2016). What Do You Mean, ‘Tipping Point’? *Trends in Ecology & Evolution*, 31(12), 902–904. <https://doi.org/10.1016/j.tree.2016.09.011>
- van Nes, E. H., Staal, A., Hantson, S., Holmgren, M., Pueyo, S., Bernardi, R. E., Flores, B. M., Xu, C., & Scheffer, M. (2018). Fire forbids fifty-fifty forest. *PLOS ONE*, 13(1), e0191027. <https://doi.org/10.1371/journal.pone.0191027>

- van Oorschot, F., van der Ent, R. J., Hrachowitz, M., & Alessandri, A. (2021). Climate-controlled root zone parameters show potential to improve water flux simulations by land surface models. *Earth System Dynamics*, *12*(2), 725–743. <https://doi.org/10.5194/esd-12-725-2021>
- Wang-Erlandsson, L., Bastiaanssen, W. G. M., Gao, H., Jägermeyr, J., Senay, G. B., van Dijk, A. I. J. M., Guerschman, J. P., Keys, P. W., Gordon, L. J., & Savenije, H. H. G. (2016). Global root zone storage capacity from satellite-based evaporation. *Hydrology and Earth System Sciences*, *20*(4), 1459–1481. <https://doi.org/10.5194/hess-20-1459-2016>
- Wieczynski, D. J., Boyle, B., Buzzard, V., Duran, S. M., Henderson, A. N., Hulshof, C. M., Kerkhoff, A. J., McCarthy, M. C., Michaletz, S. T., Swenson, N. G., Asner, G. P., Bentley, L. P., Enquist, B. J., & Savage, V. M. (2019). Climate shapes and shifts functional biodiversity in forests worldwide. *Proceedings of the National Academy of Sciences*, *116*(2), 587–592. <https://doi.org/10.1073/pnas.1813723116>
- Wilson, S. J., Coomes, O. T., & Dallaire, C. O. (2019). The ‘ecosystem service scarcity path’ to forest recovery: A local forest transition in the Ecuadorian Andes. *Regional Environmental Change*, *19*(8), 2437–2451. <https://doi.org/10.1007/s10113-019-01544-1>
- Zemp, D. C., Schleussner, C.-F., Barbosa, H. M. J., Hirota, M., Montade, V., Sampaio, G., Staal, A., Wang-Erlandsson, L., & Rammig, A. (2017). Self-amplified Amazon forest loss due to vegetation-atmosphere feedbacks. *Nature Communications*, *8*, 14681. <https://doi.org/10.1038/ncomms14681>
- Zhang, Y., Peña-Arancibia, J. L., McVicar, T. R., Chiew, F. H. S., Vaze, J., Liu, C., Lu, X., Zheng, H., Wang, Y., Liu, Y. Y., Miralles, D. G., & Pan, M. (2016). Multi-decadal trends in global terrestrial evapotranspiration and its components. *Scientific Reports*, *6*, 19124. <https://doi.org/10.1038/srep19124>
- Zhou, L., Tian, Y., Myneni, R. B., Ciais, P., Saatchi, S., Liu, Y. Y., Piao, S., Chen, H., Vermote, E. F., Song, C., & Hwang, T. (2014). Widespread decline of Congo rainforest greenness in the past decade. *Nature*, *509*(7498), 86–90. <https://doi.org/10.1038/nature13265>